Dye-sensitized solar cells based on novel donor–acceptor π-conjugated benzofuro[2,3-*c*]oxazolo[4,5-*a*]carbazole-type fluorescent dyes exhibiting solid-state fluorescence

Yousuke Ooyama, Akihiro Ishii, Yusuke Kagawa, Ichiro Imae and Yutaka Harima*

Received (in Durham, UK) 8th May 2007, Accepted 19th July 2007
First published as an Advance Article on the web 8th August 2007
DOI: 10.1039/b706896d

Novel donor–acceptor π-conjugated benzofuro[2,3-*c*]oxazolo[4,5-*a*]carbazole-type fluorescent dyes (**2a–2d**) with substituents (R = H, butyl, benzyl and 5-nonyl) on the nitrogen of carbazole ring have been designed and synthesized as sensitizers in dye-sensitized solar cells (DSSCs). Absorption and fluorescence properties of **2a–2d** are similar in solution. In the solid state, however, the dyes **2c** (R = benzyl) and **2d** (R = 5-nonyl) with bulky substituents exhibit strong solid-state fluorescence properties, which are attributed to the reduction of the π–π interaction between the dyes. Photovoltaic parameters of DSSCs based on **2a–2d** are measured with the amount of dyes adsorbed on TiO_2 film as a parameter. It is found that the **2d** exhibits a 100% efficiency for absorbed photon-to-current conversion, demonstrating that bulky substituents in **2d** can efficiently prevent intermolecular energy transfer between the dyes in molecular aggregation states.

Introduction

Dye-sensitized solar cells (DSSCs) fabricated using organic materials have attracted increasing interest because of their high abilities to convert solar light to electricity at low cost.[1–6] A large number of organic dyes have been developed and the relationship between the chemical structure and photovoltaic performance of DSSCs based on the dyes is examined. In particular, donor–acceptor π-conjugated dyes possessing broad and intense spectral features are useful as sensitizers.[2–6] Unfortunately, these dyes are liable to form π-stacked aggregates between the dyes on metal oxides such as TiO_2, which leads to reduction in electron-injection yield from the dyes to the conduction band of TiO_2 owing to intermolecular energy transfer.[5,6] In order to prevent aggregation of dye molecules on TiO_2 surface, deoxycholic acid (DCA) has been used in a number of research works.[5,7] The key point in designing of new effective donor–acceptor-type sensitizers for DSSCs is to reduce possible intermolecular energy transfer between dyes adsorbed on TiO_2 surface. The influences of molecular aggregation on the photovoltaic performances of DSSCs are not yet fully understood because of difficulty in making a systematic study of the regulation of molecular arrangement on TiO_2 surface.

In the present study, we have designed and synthesized novel donor–acceptor π-conjugated benzofuro[2,3-*c*]oxazolo-[4,5-*a*]carbazole-type fluorescent dyes (**2**). The solid-state fluorescence properties of these dyes are changed by introducing bulky substituents in the dye skeleton. The bulky groups reduce the π–π interaction between the dyes and prevent the fluorescence quenching in molecular aggregation state. It is expected that the use of these dyes as sensitizers should enable elucidation of the influence of molecular aggregation on the photovoltaic performances of DSSCs.

Department of Applied Chemistry, Graduate School of Engineering, Hiroshima University, Higashi-hiroshima, 739-8527, Japan. E-mail: harima@mls.ias.hiroshima-u.ac.jp; Fax: (+81) 82-424-5494

Results and discussion

Synthesis of benzofuro[2,3-*c*]oxazolo[4,5-*a*]carbazole-type fluorescent dyes (1a–1d) and (2a–2d)

The synthetic pathway of the dyes is shown in Scheme 1. We used 7-(4-cyanophenyl)-3-dibutylaminobenzofuro[2,3-*c*]oxazolo[4,5-*a*]carbazole **1a**[8] as a starting material. The reaction of **1a** with alkyl halide using sodium hydride gave **1b–1d** in 74–82% yields. The compounds **2a–2d** were synthesized in 68–90% yields by hydrolysis of **1a–1d**.

Spectroscopic properties of 2a–2d in solution and in the solid state

The visible absorption and fluorescence spectral data of **2a–2d** in 1,4-dioxane are summarized in Table 1 and the spectra of **2a–2d** are depicted in Fig. 1. The absorption and fluorescence spectra of the fluorescent dyes **2a–2d** closely resemble each other, showing that the effect of N-alkylation of the carbazole ring on the photophysical properties of **2** is negligible. The absorption maxima of the dyes appear at around 415 and 350 nm, and the corresponding fluorescence bands are observed at around 515 nm. The fluorescence quantum yields (Φ) of **2a–2d** are close to 100%. In the solid state, however, the fluorescent dye **2d** exhibits a stronger fluorescence band than the other compounds (Table 1). The fluorescence quantum yields increase in the order of **2d** (Φ = 0.11) > **2c** (Φ = 0.10) > **2b** (Φ = 0.04) ≫ **2a** ($\Phi \approx 0$). It was difficult to determine exactly a quantum yield of **2a** because of a feeble fluorescence intensity. These results demonstrate that the N-alkylation of

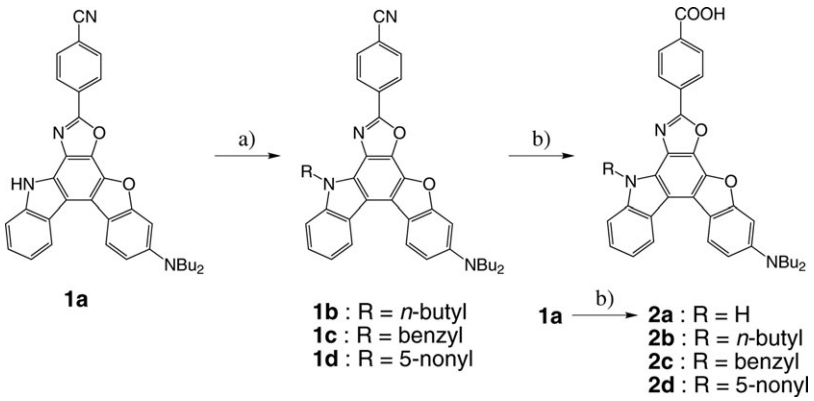

Scheme 1 Synthesis of fluorescent dyes **1a–1d** and **2a–2d**: *Reagents and conditions*: (a) NaH, alkyl halide, acetonitrile, RT, 5–24 h; (b) NaOH aq, ethanol, reflux, 16–24 h.

Table 1 Optical properties of **2a–2d** in 1,4-dioxane and in the crystalline state

	In 1,4-dioxane			In the crystalline state		
	λ_{max}^{abs}/nm (ε_{max} /dm^3 mol^{-1} cm^{-1})	λ_{max}^{fl}/nm	Φ	λ_{max}^{ex}/nm	λ_{max}^{fl}/nm	Φ
2a	416 (25 700), 347 (25 400)	525	0.97	545	582	[a]
2b	419 (26 300), 351 (29 600)	519	0.97	529	571	0.04
2c	408 (23 400), 348 (23 400)	508	0.97	508	562	0.10
2d	411 (28 700), 349 (30 900)	507	0.97	537	580	0.11

[a] Too weak to be measured.

the carbazole ring in **2a** effectively reduces the intermolecular π–π interaction such as causing the fluorescence quenching in the solid state.[9–11]

Electrochemical properties of 2a–2d and their HOMO and LUMO energy levels

The electrochemical properties of **2a–2d** were determined by cyclic voltammetry (CV) in acetonitrile containing 0.1 M Et_4NClO_4. As an example, the CV of **2d** is shown in Fig. 2. The CV curves of these compounds showed three redox waves at similar potentials irrespective of the compounds (Table 2). Three oxidation peaks of these compounds are determined to be 0.31–0.32, 0.80–0.85 and 0.97–0.99 V *vs.* Ag/Ag^+. The corresponding reduction peaks appear at 0.25–0.26 V for the first redox step and the peak separations are *ca.* 60 mV. The first oxidation and reduction peaks are clearly observed, suggesting that the first oxidized state of the dyes is stable. On the other hand, the second and third redox waves are less clear than the first one, showing a poor stability of the second and third oxidized states of the dyes.

On the bases of the spectral analyses and CVs, we estimated the HOMO and LUMO energy levels of the four dyes. The HOMO energy levels for **2a–2d** are evaluated to be 0.87, 0.88, 0.87 and 0.88 V with respect to NHE, respectively. The LUMO energy levels of the dyes are estimated from the first oxidation potential, and an intersection of absorption and fluorescence spectra (480 nm (2.58 eV), 472 (2.63), 470 (2.64) and 475 (2.61) for **2a–2d**, respectively) corresponding to the energy gap between HOMO and LUMO. They are −1.71, −1.75, −1.77 and −1.73 V for **2a–2d**, respectively. Evidently, the LUMO energy levels for these dyes are higher than the energy level of the TiO_2 conduction band (−0.5 V), showing that these dyes can inject efficiently electrons to the conduction band of the TiO_2 electrode. The results of absorption and fluorescence spectra and CV for these dyes demonstrate that all these dyes have similar HOMO and LUMO energy levels.

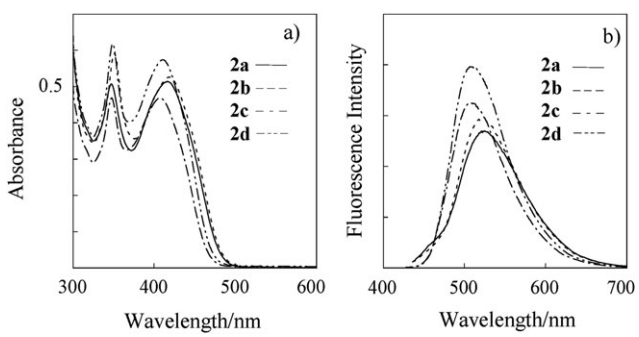

Fig. 1 (a) Absorption and (b) fluorescence spectra of **2a–2d** in 1,4-dioxane.

Semi-empirical MO calculations (AM1, INDO/S)

The photophysical and electrochemical properties of **2a–2d** were analyzed by using semi-empirical molecular orbital (MO) calculations. The molecular structures were optimized by using the MOPAC/AM1 method,[12] and then the INDO/S method[13] was used for spectroscopic calculations. The calculated absorption wavelengths and the transition characters of the first absorption bands are collected in Table 3. The observed and calculated absorption spectra of the compounds compare well with each other with respect to both the absorption wavelength and the absorption intensity, although the calculated absorption wavelengths are slightly blue-shifted. The deviation of the INDO/S calculations, giving transition

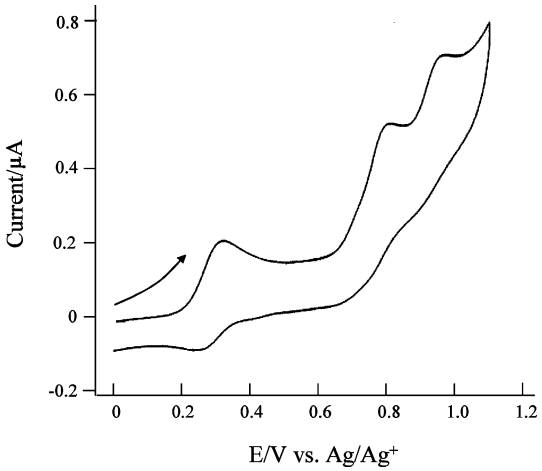

Fig. 2 Cyclic voltammogram of compound **2d** in acetonitrile containing 0.1 M Et_4NClO_4 at a scan rate of 20 mV s^{-1}. The arrow denotes the direction of the potential scan.

energies greater than the experimental values, has been generally observed.[14] The calculations show that the excitation bands of the dyes at *ca.* 400 nm are mainly assigned to a transition from HOMO to LUMO, where HOMOs are mostly localized on the 3-dibutylaminobenzofuro[2,3-*c*]oxazolo-[4,5-*a*]carbazole moiety for all dyes, and LUMOs are mostly localized on the carboxylphenyl moiety. The changes in the calculated electron density accompanying the first electron excitation are shown in Fig. 3, which reveals a strong migration of intramolecular charge transfer from the 3-dibutylaminobenzofuro[2,3-*c*]oxazolo[4,5-*a*]carbazole moiety to the carboxylphenyl moiety for all dyes. Furthermore, the calculations show that the second excitation bands of the dyes are mainly assigned to the transition from HOMO to LUMO + 1, where a moderate migration of charge from the 3-dibutylaminobenzofuro[2,3-*c*]oxazolocarbazole moiety to the carboxylphenyl moiety is also observed. These calculation results indicate that the effects of N-alkylation of the carbazole ring on the photophysical and electrochemical properties of these dyes are negligible, consistent with the experiment results of the absorption and fluorescence spectra and the CVs.

Photovoltaic performances of DSSCs based on 2a–2d

DSSCs based on **2a–2d** were prepared at different adsorption amounts of the dyes and their photovoltaic performances were evaluated for the respective DSSCs. The incident photons-to-current conversion efficiency (IPCE) spectra and photocurrent–voltage curves depicted in Fig. 4 and 5, respectively, are obtained for the DSSCs with the maximum adsorption of the dyes: 13.9×10^{16}, 7.9×10^{16}, 2.5×10^{16} and 2.3×10^{16} molecules cm^{-2} for **2a–2d**, respectively. Fig. 4 includes also the absorption spectra of the dyes **2a–2d** adsorbed on the TiO_2 electrodes. Here, IPCE is defined by the following equation:

$$\mathrm{IPCE}(\%) = \frac{1240(\mathrm{eV\,nm})J_{sc}(\lambda)(\mathrm{mA\,cm^{-2}})}{\lambda(\mathrm{nm})I(\lambda)(\mathrm{mW\,cm^{-2}})} \times 100 \qquad (1)$$

where $J_{sc}(\lambda)$ is the short-circuit photocurrent density generated by monochromatic light of a wavelength λ and $I(\lambda)$ is an intensity of the monochromatic light. The photocurrent–voltage curves of Fig. 5 are obtained under AM 1.5 irradiation (60 mW cm^{-2}). Photovoltaic performances of the DSSCs deduced from Fig. 5 are summarized in Table 1. The solar energy-to-electricity conversion yield (η(%)) is expressed by the following equation:

$$\eta(\%) = \frac{J_{sc}(\mathrm{mA\,cm^{-2}})V_{oc}(\mathrm{V})ff}{I_0(\mathrm{mW\,cm^{-2}})} \times 100 \qquad (2)$$

where I_0 is the intensity of an incident white light (60 mW cm^{-2}), V_{oc} is the open-circuit photovoltage, and *ff* represents the fill factor.

Fig. 4 shows that the absorption peak wavelengths of adsorbed dyes on TiO_2 films are similar to those in 1,4-dioxane and the maximum adsorption of the four sensitizers **2a–2d** on TiO_2 films are quite similar. However, noteworthy is that considerable differences in the onsets of absorption bands were observed between the four dyes; the onsets of absorption bands are red-shifted by 150 nm for **2a** and **2b** and 90 nm for **2c** and **2d**. Such a red-shift has been observed also in other donor–acceptor π-conjugated dyes and attributed to the dye aggregation on TiO_2 electrode.[4c,5c] On the other hand, the maximum IPCE values are very similar; 48% for **2a**, 46% for **2b**, 39% for **2c**, and 45% for **2d**, and the photocurrent–voltage curves for four dyes also closely resemble each other. As shown in Table 4, no significant differences in photovoltaic parameters are seen among the dyes, although the maximum amounts of dyes adsorbed on TiO_2 film differ considerably. The occupancy areas of **2a–2d** calculated with the maximum amounts of adsorbed dyes and a real surface area of 1470 cm^2 for 1 cm^2 geometric area of TiO_2 were 106, 186, 588 and 639 $Å^2$, respectively, indicating that the dyes **2a** and **2b** are more highly aggregated on TiO_2 surface than **2c** and **2d**.

To see explicitly the influence of the dye aggregation on the probability of charge injection from the dye to the conduction band of TiO_2, photovoltaic parameters were evaluated for DSSCs with varying adsorption amounts of the dyes. Fig. 6 depicts the peak IPCE value ($IPCE_{max}$) plotted against the light harvesting efficiency (LHE) at that wavelength for **2a** and

Table 2 Electrochemical properties of **2a–2d**

Compound	E_{pa}[a]/V (*vs.* Ag/Ag^+)	E_{pc}[b]/V (*vs.* Ag/Ag^+)	ΔE_p/mV	$E_{1/2}$/V
2a	0.31, 0.82, 0.98	0.25, —, —	60,—, —	0.28,—, —
2b	0.32, 0.85, 0.99	0.25, —, —	70,—, —	0.29,—, —
2c	0.31, 0.80, 0.97	0.25, 0.74, —	60, 60, —	0.28, 0.77, —
2d	0.32, 0.82, 0.97	0.26, 0.77, —	60, 50, —	0.29, 0.80, —

[a] E_{pa} and E_{pc} are the anodic and cathodic peak potentials in acetonitrile (0.1 M Et_4NClO_4). [b] E_{pa} and E_{pc} are the anodic and cathodic peak potentials in acetonitrile (0.1 M Et_4NClO_4).

Table 3 Calculated absorption spectra for **2a–2d**

	Absorption (calc.)		
Compound	λ_{max}/nm	f^a	CI component[b]
2a	402	0.92	HOMO → LUMO (75%)
	328	0.59	HOMO → LUMO + 1(43%)
			HOMO−1 → LUMO (13%)
2b	407	0.89	HOMO → LUMO (76%)
	331	0.61	HOMO → LUMO+1 (43%)
			HOMO−1 → LUMO (16%)
2c	405	0.87	HOMO → LUMO (76%)
	330	0.50	HOMO → LUMO+1 (34%)
			HOMO−1 → LUMO (14%)
2d	409	0.88	HOMO → LUMO (76%)
	331	0.59	HOMO → LUMO+1 (42%)
			HOMO−1 → LUMO (17%)

[a] Oscillator strength. [b] The transition is shown by an arrow from one orbital to another, followed by its percentage CI (configuration interaction) component.

2d, where LHE is defined as $1 - T$ and T means transmittance due to dyes deposited on the nanoporous TiO_2 electrode. Both of the plots appear to fit straight lines passing through the origin, suggesting that the charge injection probability is in proportion to the amount of absorbed photons for the two sorts of dyes showing highly different aggregation behaviors. A salient feature to be noted in Fig. 6 is the difference of the slope values. It is reasonable to presume that less efficient charge injection for **2a** is ascribable to stronger intermolecular π–π interactions in molecular aggregation state of **2a**. Surprisingly, the slope for **2d** is close to unity, indicating that almost all absorbed photons are converted to a current flow. This fact emphasizes that the introduction of 5-nonyl group as bulky substituent on the carbazole ring to the chromophores can efficiently prevent intermolecular energy transfer between the dyes in molecular aggregation states and lead to a higher photon-to-current conversion efficiency.

In the presence of DCA, the J_{sc} values for **2a** and **2b** were increased to 2.84 and 2.78 mA cm^{-2}, and the η values reached 1.62 and 1.49%, respectively. This shows that the co-adsorption of the DCA prevents dye aggregation and increases the electron injection yield. Dyes **2c** and **2d**, on the other hand, did not adsorb on the TiO_2 electrodes in the presence of DCA. However, for dye **2d**, the amounts of adsorbed dyes on TiO_2 film was increased to 6.5×10^{16} molecules cm^{-2}, by using a thicker TiO_2 electrode (*ca.* 10 μm). As a consequence, the $IPCE_{max}$ reached 60%, and the J_{sc} and η values were increased to 2.17 mA cm^{-2} and 1.02%, respectively. This result strongly demonstrates that the dyes **2c** and **2d** with bulky substituents can avoid effectively the molecular aggregation state even in the absence of DCA.

Conclusions

Novel donor–acceptor π-conjugated benzofuro[2,3-*c*]oxazolo[4,5-*a*]carbazole-type fluorescent dyes exhibiting solid-state fluorescence have been designed and synthesized, and photovoltaic performance of DSSCs based on these dyes are investigated. A comparison of the $IPCE_{max}$ *vs.* LHE plots for **2a** and **2d** demonstrates that bulky substituent in **2d** prevent the dye molecules from forming strong intermolecular π–π interactions in the solid state, resulting in higher photovoltaic performances. We believe that fluorescent dyes exhibiting solid-state fluorescence can be a class of potential sensitizers for DSSCs.

Experimental

Melting points were measured with a Yanaco micro melting point apparatus MP model. IR spectra were recorded on a Perkin Elmer Spectrum One FT-IR spectrometer by the ATR method. Absorption spectra were observed with a Shimadzu UV-3150 spectrophotometer and fluorescence spectra were measured with a Hitachi F-4500 spectrophotometer. The fluorescence quantum yields were determined by a Hamamatsu C9920-01 equipped with CCD by using a calibrated integrating sphere system (λ_{ex} = 325 nm). Cyclic voltammograms were recorded in MeCN–Et_4NClO_4 (0.1 M) solution with a three-electrode system consisting of Ag/Ag^+ as reference electrode, Pt plate as working electrode, and Pt wire as counter electrode, by using a Hokuto Denko HAB-151 potentiostat equipped with a functional generator. Elemental analyses were made with a Perkin Elmer 2400 II CHN analyzer. ^1H NMR spectra were taken on a JNM-LA-400 (400 MHz) FT NMR spectrometer with tetramethylsilane (TMS) as an internal standard. Column chromatography

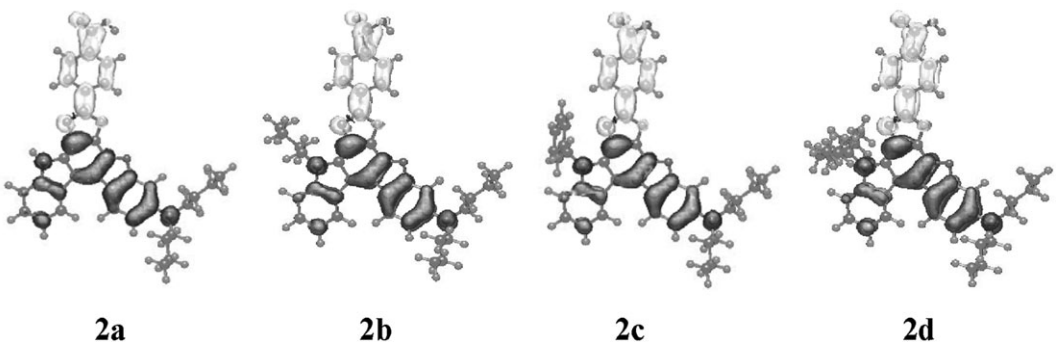

Fig. 3 Calculated electron density changes accompanying the first electronic excitation of **2a–2d**. The black and white lobes signify decrease and increase in electron density accompanying the electronic transition. Their areas indicate the magnitude of the electron density change.

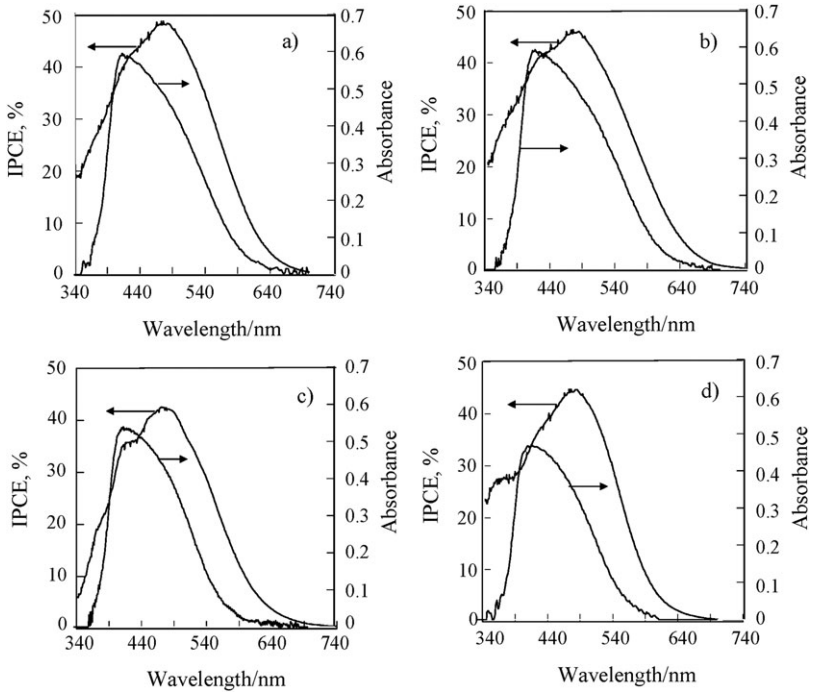

Fig. 4 Absorption spectra of the dyes adsorbed on TiO_2 film and the IPCE spectra for DSSCs based on the dyes; (a) **2a**, (b) **2b**, (c) **2c** and (d) **2d**. The amounts of adsorbed dyes on TiO_2 film are 13.9×10^{16}, 7.9×10^{16}, 2.5×10^{16} and 2.3×10^{16} molecules cm^{-2} for **2a**, **2b**, **2c** and **2d**, respectively. The 7 μm thick TiO_2 electrodes were used.

was performed on silica gel (KANTO CHEMICAL, 60 N, spherical, neutral).

Synthesis of 9-butyl-7-(4-cyanophenyl)-3-dibutylaminobenzofuro[2,3-*c*]oxazolo[4,5-*a*]carbazole (1b)

A solution of **1a** (1.0 g, 1.90 mmol) in dry acetonitrile was treated with sodium hydride (60%, 0.23 g, 5.70 mmol) and stirred for 1 h at room temperature. Iodobutane (1.75 g, 9.49 mmol) was added in dropwise manner over 30 min and the solution was stirred at room temperature for 5 h. After concentrating under reduced pressure, the resulting residue was dissolved in CH_2Cl_2, and washed with water. The organic extract was dried over $MgSO_4$, filtered, and concentrated. The residue was chromatographed on silica gel (CH_2Cl_2 as eluent) to give **1b** (0.91 g, yield 82%); mp 230–231 °C; IR (KBr): $\tilde{\nu}$ = 2163 cm^{-1}; ^1H NMR ($CDCl_3$, TMS) δ 1.00–1.03 (9H, m), 1.42–1.68 (10H, m), 2.00 (2H, m), 3.42 (4H, t), 4.92 (2H, t), 6.87 (1H, dd, J = 8.70 and 2.20 Hz), 6.92 (1H, m, J = 2.20 Hz), 7.37–7.41 (1H, m), 7.53–7.57 (1H, m), 7.77 (2H, d, J = 8.21 Hz), 8.10 (1H, d, J = 8.22 Hz), 8.33 (2H, d, J = 8.21 Hz), 8.42 (1H, d, J = 8.70 Hz), 8.62 (1H, d, J = 7.73 Hz); elemental analysis: calc. (%) for $C_{38}H_{38}N_4O_2$: C 78.32, H 6.57, N 9.61; found: C 78.22, H 6.44, N 9.61.

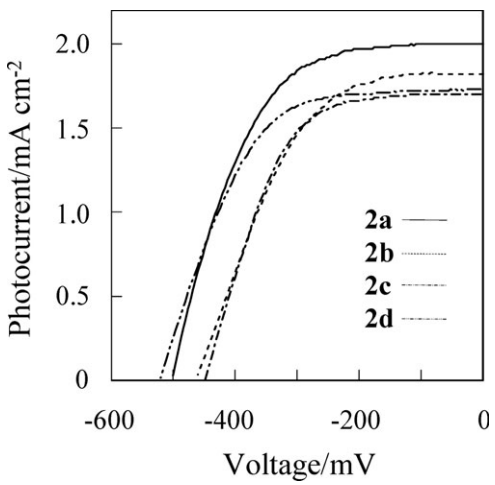

Fig. 5 Photocurrent–voltage curves of the same DSSCs as those used in Fig. 4.

Synthesis of 9-benzyl-7-(4-cyanophenyl)-3-dibutylaminobenzofuro[2,3-*c*]oxazolo[4,5-*a*]carbazole (1c)

A solution of **1a** (1.0 g, 1.90 mmol) in dry acetonitrile was treated with sodium hydride (60%, 0.23 g, 5.70 mmol) and stirred for 1 h at room temperature. Benzyl bromide (1.62 g, 9.49 mmol) was added in dropwise manner over 30 min and the solution was stirred at room temperature for 10 h. After concentrating under reduced pressure, the resulting residue was dissolved in CH_2Cl_2, and washed with water. The organic

Table 4 Photovoltaic parameters of DSSCs based on **2a–2d**

Dye	J_{sc}/mA cm^{-2}	V_{oc}/mV	*ff*	η (%)	Molecules cm^{-2} [a]/10^{16}
2a	2.00	504	0.54	0.89	13.9
2b	1.82	464	0.52	0.72	7.9
2c	1.67	452	0.60	0.74	2.5
2d	1.73	536	0.58	0.88	2.3

[a] Adsorption amount per unit area of TiO_2 film.

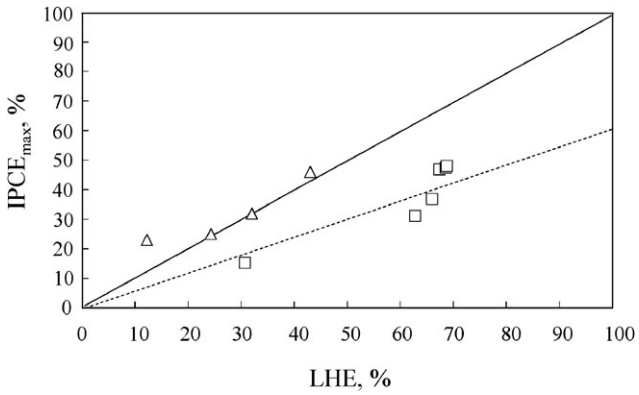

Fig. 6 Plots of $IPCE_{max}$ against LHE for **2a** (□) and **2d** (△).

extract was dried over $MgSO_4$, filtered, and concentrated. The residue was chromatographed on silica gel (CH_2Cl_2 as eluent) to give **1c** (0.93 g, yield 79%); mp 253–254 °C; IR (KBr): $\tilde{\nu}$ = 2229 cm^{-1}; ^1H NMR (acetone-d_6, TMS) δ 1.04 (6H, t), 1.47–1.53 (4H, m), 1.72–1.76 (4H, m), 3.51–3.56 (4H, m), 6.37 (2H, s), 7.03–7.07 (3H, m), 7.20–7.28 (3H, m), 7.39–7.54 (3H, m), 7.78 (1H, d, J = 7.60 Hz), 8.06 (2H, d, J = 8.80 Hz), 8.52–8.57 (3H, m), 8.76 (1H, d, J = 7.60 Hz); elemental analysis: calc. (%) for $C_{41}H_{36}N_4O_2$: C 79.84, H 5.88, N 9.08; found: C 79.66, H 5.85, N 8.86.

Synthesis of 9-(5-nonyl)-7-(4-cyanophenyl)-3-dibutylaminobenzofuro[2,3-*c*]oxazolo[4,5-*a*]carbazole (1d)

A solution of **1a** (1.0 g, 1.90 mmol) in dry acetonitrile was treated with sodium hydride (60%, 0.23 g, 5.70 mmol) and stirred for 1 h at room temperature. 5-Bromononane (1.62 g, 9.49 mmol) was added in dropwise manner over 30 min and the solution was stirred at room temperature for 24 h. After concentrating under reduced pressure, the resulting residue was dissolved in CH_2Cl_2, and washed with water. The organic extract was dried over $MgSO_4$, filtered, and concentrated. The residue was chromatographed on silica gel (CH_2Cl_2 as eluent) to give **1d** (0.92 g, yield 74%); mp 156–158 °C; IR (KBr): $\tilde{\nu}$ = 2227 cm^{-1}; ^1H NMR (acetone-d_6, TMS) δ 0.72 (6H, t), 0.85–0.90 (4H, m), 1.03 (6H, t), 1.26–1.51 (12H, m), 1.68–1.74 (4H, m), 3.50 (4H, t), 4.95–4.98 (1H, m), 6.96–7.00 (2H, m), 7.39–7.52 (2H, m), 7.95–8.05 (3H, m), 8.50–8.52 (3H, m), 8.74 (1H, d, J = 7.56 Hz); elemental analysis: calc. (%) for $C_{43}H_{48}N_4O_2$: C 79.11, H 7.41, N 8.58; found: C 78.81, H 7.64, N 8.28.

7-(4-Carboxyphenyl)-3-dibutylaminobenzofuro[2,3-*c*]oxazolo[4,5-*a*]carbazole (2a)

A solution of **1a** (1.0 g, 1.90 mmol) in ethanol (500 ml) was added in dropwise aqueous NaOH (0.76 g, 19 mmol, 50 mL) with stirring under reflux. After further stirring for 16 h under reflux, the solution was acidified to pH 4 with 2 N HCl, and concentrated under reduced pressure. The residue was dissolved in CH_2Cl_2, and washed with water. The organic extract was dried over $MgSO_4$, filtered, and concentrated. The residue was chromatographed on silica gel (CH_2Cl_2–ethyl acetate = 2 : 5 as eluent) to give **2a** (0.91 g, yield 88%); mp 296–297 °C (decomposition); IR (KBr): $\tilde{\nu}$ = 3240, 1692 cm^{-1}; ^1H NMR (DMSO-d_6, TMS) δ 0.97 (6H, t), 1.37–1.43 (4H, m), 1.58–1.63 (4H, m), 3.38 (4H, t) overlap peak of dissolved water in DMSO-d_6, 6.94–6.96 (1H, m), 7.03–7.05 (1H, m), 7.33–7.38 (1H, m), 7.46–7.50 (1H, m), 7.66 (1H, d, J = 8.08 Hz), 8.20 (2H, d, J = 8.32 Hz), 8.38 (2H, d, J = 8.32 Hz), 8.46 (1H, d, J = 8.32 Hz), 8.60 (1H, d, J = 7.84 Hz), 12.50 (1H, s, NH); elemental analysis: calc. (%) for $C_{34}H_{31}N_3O_4$: C 74.84, H 5.73, N 7.70; found: C 74.72, H 5.63, N 7.67.

9-Butyl-7-(4-carboxyphenyl)-3-dibutylaminobenzofuro[2,3-*c*]oxazolo[4,5-*a*]carbazole (2b)

A solution of **1b** (0.10 g, 0.17 mmol) in ethanol (500 ml) was added in dropwise aqueous NaOH (0.089 g, 1.72 mmol, 50 mL) with stirring under reflux. After further stirring for 24 h under reflux, the solution was acidified to pH 4 with 2 M HCl, and concentrated under reduced pressure. The residue was dissolved in CH_2Cl_2, and washed with water. The organic extract was dried over $MgSO_4$, filtered, and concentrated. The residue was chromatographed on silica gel (CH_2Cl_2–ethyl acetate = 5 : 1 as eluent) to give **2b** (0.093 g, yield 90%); mp 301–302 °C; IR (KBr): $\tilde{\nu}$ = 1693 cm^{-1}; ^1H NMR (DMSO-d_6, TMS) δ 0.97 (3H, t), 1.04 (6H, t), 1.23–1.26 (2H, m), 1.37–1.41 (4H, m), 1.59–1.63 (4H, m), 1.92–1.97 (2H, m), 4.39 (4H, t), 5.01 (2H, t), 6.94–7.06 (2H, m), 7.37–7.41 (1H, m), 7.53–7.57 (1H, m), 7.83 (1H, d, J = 8.28 Hz), 8.17–8.20 (2H, m), 8.36–8.38 (2H, m), 8.47–8.49 (1H, m), 8.64 (1H, d, J = 8.28 Hz); elemental analysis: calc. (%) for $C_{38}H_{39}N_3O_4$: C 75.85, H 6.53, N 6.98; found: C 75.76, H 6.70, N 6.90.

9-Benzyl-7-(4-carboxyphenyl)-3-dibutylaminobenzofuro[2,3-*c*]oxazolo[4,5-*a*]carbazole (2c)

A solution of **1c** (0.10 g, 0.16 mmol) in ethanol (500 ml) was added in dropwise aqueous NaOH (0.091 g, 1.16 mmol, 50 mL) with stirring under reflux. After further stirring for 24 h under reflux, the solution was acidified to pH 4 with 2 M HCl, and concentrated under reduced pressure. The residue was dissolved in CH_2Cl_2, and washed with water. The organic extract was dried over $MgSO_4$, filtered, and concentrated. The residue was chromatographed on silica gel (CH_2Cl_2 as eluent) to give **2c** (0.079 g, yield 77%); mp 250–251 °C; IR (KBr): $\tilde{\nu}$ = 1647 cm^{-1}; ^1H NMR (acetone-d_6, TMS) δ 1.04 (6H, t), 1.47–1.53 (4H, m), 1.72–1.76 (4H, m), 3.51–3.55 (4H, m), 6.00 (2H, s), 7.01–7.07 (3H, m), 7.20–7.28 (3H, m), 7.40–7.48 (3H, m), 7.78 (1H, d, J = 7.60 Hz), 8.19 (2H, d, J = 8.40 Hz), 8.43 (2H, d, J = 8.40 Hz), 8.53 (1H, d, J = 8.80 Hz), 8.71 (1H, d, J = 7.60 Hz); elemental analysis: calc. (%) for $C_{41}H_{37}N_3O_4$: C 77.46, H 5.87, N 6.61; found: C 77.35, H 6.02, N 6.78.

9-(5-Nonyl)-7-(4-carboxyphenyl)-3-dibutylaminobenzofuro[2,3-*c*]oxazolo[4,5-*a*]carbazole (2d)

A solution of **1c** (0.15 g, 0.23 mmol) in ethanol (500 ml) was added in dropwise aqueous NaOH (0.13 g, 2.30 mmol, 50 mL) with stirring under reflux. After further stirring for 24 h under reflux, the solution was acidified to pH 4 with 2 M HCl, and concentrated under reduced pressure. The residue was

dissolved in CH_2Cl_2, and washed with water. The organic extract was dried over $MgSO_4$, filtered, and concentrated. The residue was chromatographed on silica gel (CH_2Cl_2 as eluent) to give **2d** (0.105 g, yield 68%); mp 118–118 °C; IR (KBr): $\tilde{\nu}$ = 1690 cm^{-1}; ^1H NMR (acetone-d_6, TMS) δ 0.71 (6H, t), 1.03 (6H, t), 1.18–1.88 (18H, m), 3.50 (4H, t), 5.10–5.15 (1H, m), 7.02 (1H, d, J = 2.20 and 8.80 Hz), 7.06 (1H, d, J = 2.20 Hz), 7.41–7.45 (1H, m), 7.49–7.53 (1H, m), 7.96 (1H, d, J = 8.28 Hz), 8.23 (2H, d, J = 8.56 Hz), 8.49 (2H, d, J = 8.56 Hz), 8.59 (1H, d, J = 8.80 Hz), 8.79 (1H, d, J = 8.28 Hz); elemental analysis: calc. (%) for $C_{43}H_{49}N_3O_4$: C 76.87, H 7.35, N 6.25; found: C 76.72, H 7.38, N 6.15.

Computational methods

The semi-empirical calculations were carried out with the WinMOPAC Ver. 3 package (Fujitsu, Chiba, Japan). Geometry calculations in the ground state were made using the AM1 method.[12] All geometries were completely optimized (keyword PRECISE) by the eigenvector following routine (keyword EF). Experimental absorption spectra of the four compounds were compared with their absorption data by the semi-empirical method INDO/S (intermediate neglect of differential overlap/spectroscopic).[13] All INDO/S calculations were performed using single excitation full SCF/CI (self-consistent field/configuration interaction), which includes the configuration with one electron excited from any occupied orbital to any unoccupied orbital, where 225 configurations were considered [keyword CI (15 15)].

Preparation of the dye-sensitized solar cells based on dyes 2a–2d

The TiO_2 electrodes used for dye-sensitized solar cells were prepared as follows. Into a powder (1.30 g) of TiO_2 (P-25, d = 30–40 nm) in mortar was added water (1.9 mL) in six portions with rapid stirring. Then, three drops of 12 M nitric acid and poly(ethylene glycol) (80 mg) were successively added, and the mixture was well kneaded to a smooth paste. It was then applied on a fluorine-doped-tin-oxide (FTO) substrate and sintered for 30 min at 500 °C. The 7 μm thick TiO_2 electrode (0.5 × 0.5 cm^2 in photoactive area) was immersed into a 0.3 mM acetonitrile solution (with or without 20 mM DCA) of the dye for a number of hours enough to adsorb the photosensitizer. The DSSCs were fabricated by using the TiO_2 electrode thus prepared, Pt-coated glass as a counter electrode, and a solution of 0.05 M iodine, 0.1 M lithium iodide and 0.6 M 1,2-dimethyl-3-*n*-propylimidazolium iodide in acetonitrile as electrolyte. The photocurrent–voltage characteristics were measured using a potentiostat under a simulated solar light (AM 1.5, 60 mW cm^{-2}). IPCE spectra were measured under monochromatic irradiation with a tungsten-halogen lamp and a monochromator. BET surface areas of the TiO_2 particles were 73.5 m^2 g^{-1}. Consequently, the total area for 1 cm^2 geometric area of the film was *ca.* 1470 cm^2 for 7 μm thick TiO_2 films. Absorption spectra of the dye-adsorbed TiO_2 films were measured in the diffuse-reflection mode by a JASCO UV-VIS spectrophotometer with a calibrated integrating sphere system ISV-469. The dye-coated film was immersed in a mixed solvent of THF–DMF–NaOH aq 1 M (5 : 4 : 1), which was used to determine the amount of dye molecules adsorbed onto the film by measuring the absorbance. The quantification of each dye was made based on the λ_{max} and the molar extinction coefficient of each dye in the above solution.

Acknowledgements

We are grateful to Dr N. Koga (Hiroshima University) for the measurement of absorption spectra of the dyes adsorbed on TiO_2 film. This work was supported by a Grant-in-Aid for Scientific Research (B) (19350094) and a Grant-in-Aid for Young Scientist (B) (18750174) from the Ministry of Education, Science, Sports and Culture of Japan and by Electric Technology Research Foundation of Chugoku.

References

1 B. O'Regan and M. Grätzel, *Nature*, 1991, **353**, 737.
2 (*a*) Q.-H. Yao, F.-S. Meng, F.-Y. Li, H. Tian and C.-H. Haung, *J. Mater. Chem.*, 2003, **13**, 1048; (*b*) Y.-S. Chen, C. Li, Z.-H. Zeng, W.-B. Wang, X.-S. Wang and B.-W. Zhang, *J. Mater. Chem.*, 2005, **15**, 246; (*c*) K. R. J. Thomas, J. T. Lin, Y.-C. Hsu and K.-C. Ho, *Chem. Commun.*, 2005, 4098; (*d*) D. P. Hagberg, T. Edvinsson, T. Marinado, G. Boschloo, A. Hagfeld and L. Sun, *Chem. Commun.*, 2006, 2245.
3 T. Horiuchi, H. Miura, K. Sumioka and S. Uchida, *J. Am. Chem. Soc.*, 2004, **126**, 12218.
4 (*a*) K. Hara, K. Sayama, Y. Ohga, A. Shinpo, S. Suga and H. Arakawa, *Chem. Commun.*, 2001, 569; (*b*) K. Hara, M. Kurashige, S. Ito, A. Shinpo, S. Suga, K. Sayama and H. Arakawa, *Chem. Commun.*, 2003, 252; (*c*) K. Hara, M. Kurashige, Y. Dan-oh, C. Kasada, A. Shinpo, S. Suga, K. Sayama and H. Arakawa, *New J. Chem.*, 2003, **27**, 783.
5 (*a*) Z.-S. Wang, F.-Y. Li, C.-H. Hang, L. Wang, M. Wei, L.-P. Jin and N.-Q. Li, *J. Phys. Chem. B*, 2000, **104**, 9676; (*b*) A. Ehret, L. Stuhl and M. T. Spitler, *J. Phys. Chem. B*, 2001, **105**, 9960; (*c*) K. Hara, T. Sato, R. Katho, A. Furube, Y. Ohga, A. Shinpo, S. Suga, K. Sayama, H. Sugihara and H. Arakawa, *J. Phys. Chem. B*, 2003, **107**, 597.
6 S.-L. Li, K.-J. Jiang, K.-F. Shao and L.-M. Yang, *Chem. Commun.*, 2006, 2792.
7 A. Kay and M. Grätzel, *J. Phys. Chem.*, 1993, **97**, 6272.
8 (*a*) Y. Ooyama and Y. Harima, *Chem. Lett.*, 2006, 902; (*b*) Y. Ooyama, Y. Kagawa and Y. Harima, *Eur. J. Org. Chem.*, 2007, 3613.
9 (*a*) K. Yoshida, Y. Ooyama, H. Miyazaki and S. Watanabe, *J. Chem. Soc., Perkin Trans. 2*, 2002, 700; (*b*) Y. Ooyama, T. Nakamura and K. Yoshida, *New J. Chem.*, 2005, **29**, 447; (*c*) Y. Ooyama, T. Okamoto, T. Yamaguchi, T. Suzuki, A. Hayashi and K. Yoshida, *Chem.–Eur. J.*, 2006, 7827.
10 (*a*) K. Yoshida, Y. Ooyama, S. Tanikawa and S. Watanabe, *J. Chem. Soc., Perkin Trans. 2*, 2002, 708; (*b*) Y. Ooyama and K. Yoshida, *New J. Chem.*, 2005, **29**, 1204.
11 H. Langhals, T. Potrawa, H. Nöth and G. Linti, *Angew. Chem., Int. Ed. Engl.*, 1989, **28**, 478.
12 (*a*) J. E. Ridley and M. C. Zerner, *Theor. Chim.Acta*, 1973, **32**, 111; (*b*) J. E. Ridley and M. C. Zerner, *Theor. Chim. Acta*, 1976, **42**, 223; (*c*) A. D. Bacon and M. C. Zerner, *Theor. Chim. Acta*, 1979, **53**, 21.
13 M. J. S. Dewar, E. G. Zoebisch, E. F. Healy and J. J. Stewart, *J. Am. Chem. Soc.*, 1985, **107**, 389.
14 (*a*) M. Adachi, Y. Murata and S. Nakamura, *J. Org. Chem.*, 1993, **58**, 5238; (*b*) W. M. F. Fabian, S. Schuppler and O. S. Wolfbesis, *J. Chem. Soc., Perkin Trans. 2*, 1996, 853.

